Residual ultimate strength of damaged seamless metallic pipelines with combined dent and metal loss

Cai, Jie; Jiang, Xiaoli; Lodewijks, Gabriel; Pei, Zhiyong; Wu, Weiguo

DOI
10.1016/j.marstruc.2018.05.006

Publication date
2018

Document Version
Final published version

Published in
Marine Structures

Marine Structures 61 (2018) 188–201

Contents lists available at ScienceDirect

Marine Structures

journal homepage: www.elsevier.com/locate/marstruc

Residual ultimate strength of damaged seamless metallic pipelines with combined dent and metal loss

Jie Cai[a,*], Xiaoli Jiang[a], Gabriel Lodewijks[b], Zhiyong Pei[c], Weiguo Wu[c]

[a] Department of Maritime and Transport Technology, Delft University of Technology, 2628 CD, Delft, the Netherlands
[b] School of Aviation, University of New South Wales, NSW, 2052, Sydney, Australia
[c] Departments of Naval Architecture, Ocean and Structural Engineering, School of Transportation, Wuhan University of Technology, PR China

ARTICLE INFO

Keywords:
Metallic pipelines
Combined dent and metal loss
Residual ultimate strength
Residual stress
Nonlinear FEM
Pipe tests

ABSTRACT

The combination damage induced by mechanical interference, in reality, is more likely to happen. In this paper, numerical models on pipes with combined dent and metal loss in terms of a notch are developed and validated through tests (diameter-to-thickness ratio D/t of test pipes around 21), capable of predicting the residual ultimate strength of pipes in terms of bending moment (M_{cr}) and critical curvature (κ_{cr}). The effect of residual stress is explored, assuming a linear distribution in the pipe hoop direction. Investigations of damaged pipes with different D/t (15–50) are carried out. Through changing damage parameters in the combinations, i.e. dent depth (d_d) or metal loss depth (d_m), the corresponding effects of damage are clarified. Results show that the combined dent and notch damage is a more severe type of damage on pipe strength compared with other damage types (excluding fracture). The dent in combined damage plays a more dominant role on the pipe residual strength. Empirical formulas are proposed to predict residual ultimate strength of damaged metallic pipes (D/t around 21) with combined dent and metal loss under bending moment, which can be used for practical purposes. The application domain can be expanded to pipes with D/t up to 30 based on simulations.

1. Introduction

In the former research of the authors [1–3], a four-point bending test has been successfully carried out on metallic seamless pipes with different types of structural damage. Influential parameters such as materials, test boundaries and initial imperfections have been identified. Empirical equations were proposed for each single type of damage including a dent [3,4] and a notch [5]. As a consecutive study in this project, the present paper concentrates on the effect of combined dent and metal loss in terms of a notch accordingly.

In the industry of pipelines, structural damage in terms of a dent, metal loss, a crack and their combinations thereof is unavoidable due to mechanical interference [2,6–8]. Approximately, 23% of all the reported structural damage on pipelines in US in the past 20 years was caused by mechanical interference [9]. They may be in reality the scenarios such as excavations, dropped foreign objects, dragging anchors, collision of underwater fishing equipment, sinking vessels and even mudslides on the sea bottom [10,11]. Under these circumstances, combinations of damage are more likely to happen due to the impact randomness of the accidental scenarios. Therefore, particular attention should be paid to this type of structural damage.

The occurrence of damage on pipes indicates a degradation of performance. On the one hand, it can merely have an aesthetic

* Corresponding author.
E-mail address: J.Cai-2@tudelft.nl (J. Cai).

https://doi.org/10.1016/j.marstruc.2018.05.006
Received 12 February 2018; Received in revised form 4 May 2018; Accepted 23 May 2018
Available online 18 June 2018

Nomenclature

δ_0	amplitude of initial imperfection [mm]
κ_0	referential curvature of pipe [1/m]
κ_i	critical curvature of intact pipe (either from test or simulation) [1/m]
κ_{cr}	critical curvature [1/m]
λ_l	normalized damage length (either dent or notch)
λ_w	normalized damage width (either dent or notch)
λ_{cl}	half-wave length of cylindrical shell
σ_y	material yield stress [MPa]
θ_d	rotation angle of dent [degree]
θ_m	rotation angle of metal loss [degree]
D	outer diameter of pipe [mm]
d_d	dent depth [mm]
d_m	metal loss depth [mm]
l_m	metal loss length [mm]
M_i	ultimate bending moment of intact pipe (either from test or simulation) [kNm]
M_y	plastic bending moment [kNm]
M_{cr}	residual ultimate bending moment [kNm]
R_a	pipe average radius [mm], expressed as $R_a = (D - t)/2$
t	pipe thickness [mm]

effect such as the discoloring of the pipe coating, but on the other hand, the damage can also induce severe consequences of structures such as local buckling of pipes, overall failure, and oil/gas leaking. Incidents in pipelines with such severe consequences can be categorized as the so-called "significant incidents", which will produce a considerable loss of assets and even human life. According to the reported data from Pipeline and Hazardous Materials Safety Administration [9], within all the 11459 reported pipe incidents on liquids transmission pipelines (both onshore and offshore) with structural damage, the number of the "significant incident" was between 41% and 53%. Therefore, sufficient residual ultimate strength is of crucial importance so that the damaged pipes can continue to withstand loads in a hostile environment after suffering with damage.

The past few decades have witnessed a considerable amount of research on the ultimate strength of metallic pipes. Park and Kyriakides [12] investigated the collapse capacity of dented pipes under external pressure. Bjørnøy et al. [10] studied the bursting capacity of a dented pipe subjected to internal pressure through tests. Levold et al. [13] conducted a test on a damaged pipe with D/t of 26.5, where corrosion damage in terms of gouge was artificially introduced in the inner surface of the pipe by Electrical Discharge Machining (EDM) method. Furthermore, Bai and Bai [14] proposed some empirical equations for pipe strength prediction when pipes were subjected to pure bending. Experimentally, Es et al. [15] investigated ultimate strength of pipes without structural damage subjected to a bending moment, deploying spiral-welded steel tubes with 42-inch-diameter and D/t between 65 and 120. Based on the test results, Vasilikis et al. [16] conducted a consecutive numerical investigation.

However, no research on the residual ultimate strength of damaged pipes with combined dent and metal loss has been found so far. As a result, the objective of this paper is to quantify the residual ultimate strength of seamless pipes with combined dent and metal loss in terms of a notch subjected to bending.

The structure of this paper is arranged as follows. Section 2 describes the finite element models that will be used for the following simulations, and illustrates the definition of combined dent and metal loss damage in this paper. Then, the numerical models are compared and validated through test results in terms of failure mode and bending-curvature diagrams in Section 3. In Section 4, an initial exploration of the effect of residual stress is conducted based on assumed distribution in the pipe hoop direction. Through a series of numerical simulations using the validated model, empirical formulas are proposed in Section 5. Simulations of damaged pipes with different D/t (15–50) are also carried out for comparisons, which is used to expand the application domain of the proposed formulas. Finally, concluding remarks are made.

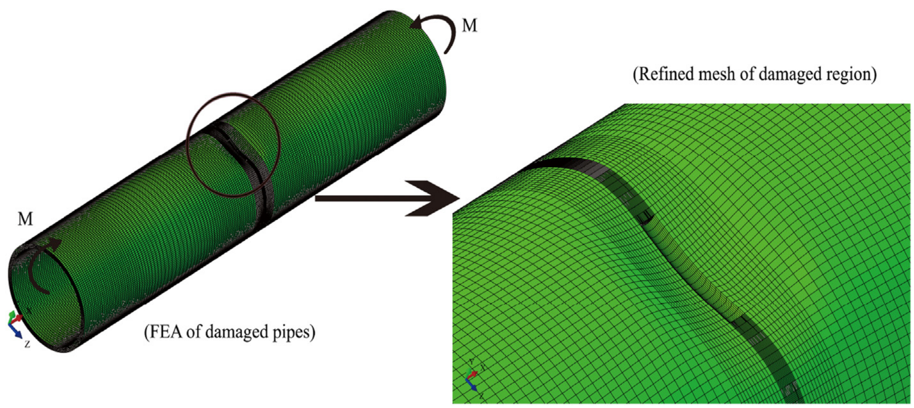

Fig. 1. FEM model of pipes with a combination of a dent and a notch.

2. Finite element models

The numerical model with an overall of 248000 elements, accounting for combined damage, has been developed in ABAQUS/Standard [17] through python script, as seen in Fig. 1. Newton-Raphson iterative method is used for numerical solutions, tracing the ultimate limit point of damaged pipe structures. The isotropic hardening of the material and the Von Mises yield criterion are used in the numerical simulation. The detailed stress-strain relationship is fitted through the measured material properties from tests. The fitting method has been described in the former research of the authors [18]. For clarity reason, the curve is not listed in this paper. A three dimensional element C3D8R is used in the numerical model. Due to the large disturbance from combined damage, initial imperfection has not been accounted for any more. Besides, no symmetry is considered in the numerical model due to the existing of structural damage.

A simplified model has been deployed based on the test set-up, removing the contact segments between specimen and strips in the test (Fig. 2) for the sake of simulation efficiency. Instead, a simplify-supported boundary condition has been used, and two referential nodes have been introduced to represent the loading location of specimen in test, exerting an equivalent forced rotation through the reference points. An overall forced displacement (1 radian) is designated in order to mimic the bending load. As described in the former paper of the authors [5], the discrepancy induced by the boundary simplification exists but is small, 1% for the ultimate bending moment and less than 7% for critical curvature.

A mesh sensitivity study is conducted for the numerical model. As seen in Fig. 1, the general mesh size in pipe hoop direction is 3 mm, less than 7% of one half-wave length ($\lambda_{cl} = 1.728\sqrt{Rt}$ [19]), while the general mesh size in pipe longitudinal direction is from 4 mm (9%λ_{cl}) to 9 mm (20%λ_{cl}) with a double bias mesh strategy. Meanwhile, the mesh is largely refined in the damaged region, with the maximum mesh size equal to 0.5 mm, i.e. less than 1.2% of one half-wave length (λ_{cl}) of cylindrical shells. The number of elements are only allowed to increase for places that are not suitable to assign a specific mesh seed. Six layers of element in thickness direction are deployed to guarantee the simulation accuracy. In order to avoid a possible hourglass caused by the using of C3D8R element, a comparison between structural energies (AllAE (all the artificial strain energy of structures) and ALLIE (all the internal energy of structures)) has been made for each simulation case. The comparison result between ALLAE and ALLIE is less than 1%, which demonstrates a trivial hourglass effect [17].

Fig. 3 shows the sketch of a combination of a dent and a notch on pipe surface. For a notch, the notch length (l_m) is the chord length of the remaining sector in the damaged pipe cross-section, while the notch depth (d_m) locates in the central axis of the damaged cross-section. There is a practical reason for this definition. In general, the on-site measurement of a straight line is much easier and more accurate than the measurement of an arc length after the occurrence of damage. Only a notch with rotation angle (θ_m) of 90^o is considered. It should be noted that the definitions of θ_m and θ_d conform to the former research of the authors [3–5]. When the damage length is along the pipe hoop direction, it is considered as 90^o. In spite of the situation that the notch will be changed a little due to the existing of dents, it is assumed that such a dent induced deformation can seldom affect the notch, for instance, its depth and its regular shape. The definition of a dent is the same with the one in the former research on dent from the authors [3,4]. Due to the largest effect of a dent with the rotation angle (θ_d) of 90^o, we only considered the dent length (l_d) along the pipe hoop direction in this paper. Fig. 4 shows the combined dent and notch damage from both the test and numerical models.

3. Validation of the finite element model

In this section, the structural behaviors of specimens with combined damage in test are simulated through the developed model from the previous section. The material properties from the material tensile test of the authors [1] are used, having a yield stress of 400 MPa, an ultimate tensile stress of 583 MPa and the maximum elongation of 22.6%. For the validation of the finite element model, the test data have been compared with the simulation results in terms of structural failure modes, bending moment-curvature

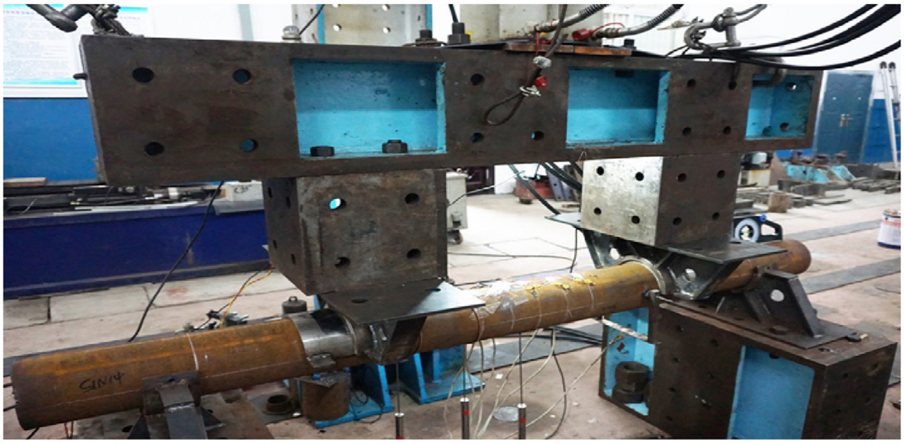

Fig. 2. Configuration of a four-point bending test in the laboratory [1].

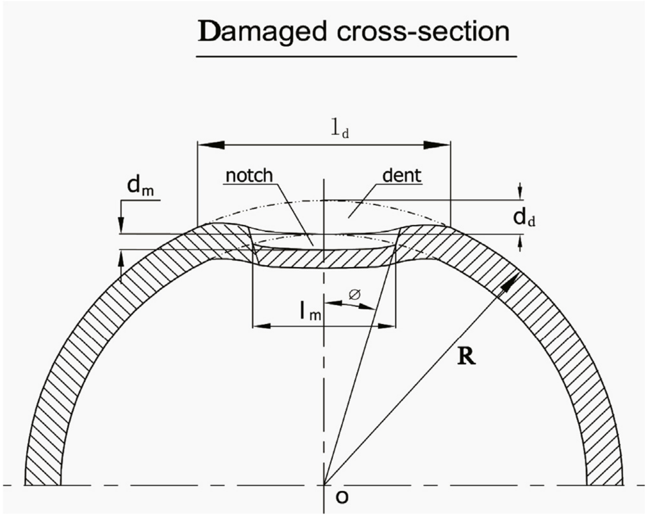

Fig. 3. Sketch of combined dent and notch damage on pipe surface (damaged cross-section).

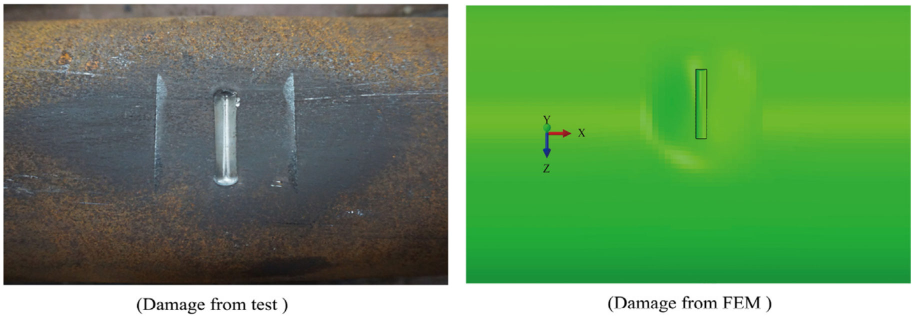

Fig. 4. Combined dent and metal loss damage from both test and numerical model.

diagrams and strength capacity.

A brief description of the four-point bending tests is first presented [1]. The designed four-point bending test set-up has been shown in Fig. 2. The specimen in the test is a seamless pipe made of Q345 [20], which is a typical material for transmission pipes with the minimum yield stress of 345 *MPa*. In this test, the overall length of each specimen was 2200 *mm* with a length of 800 *mm* under pure bending. The D/t ratio of all the specimens was around 21 with a nominal pipe thickness of 8 *mm* and a nominal pipe outer diameter of 168.3 *mm*. Before the strength test, the structural damage was introduced properly on each specimen, locating at the center of the specimen. For the introduction of combined dent and metal loss damage on specimens, the metal loss in terms of a notch was first fabricated by a machining method, and then the dent with different rotational angle was produced through a quasi-static indentation. A special indentor with a particular bulge was designed and fabricated so that the existing notch would not be largely affected during the production of the dent. The specimens (S5N1 and S5N2, as shown in Table 1) with combined damage from the test are deployed for the following comparisons.

For a comparison of the results, the bending moment (M) is normalized by the plastic bending moment ($M_y = 4R_a^2 t\sigma_y$), while the curvature (κ) is normalized by the curvature-like expression ($\kappa_0 = t/4R_a^2$). Only global curvature in the simulation is selected for comparison for the sake of accuracy. The selected locations for the calculation of the global curvature in the numerical simulation are the same as used for the tests. The bending moment in simulation is the resultant of all node forces multiplied by their corresponding force arms in the central cross-section of specimens.

Table 1
Overview of specimens with combined damage (Dimension unit: mm; Compression side; Damage size: $l_{(i)} \times w_{(i)} \times d_{(i)}$, (i) indicates different types of damage including a dent (by d), a notch (by m) and a crack (by c) respectively).

S.N.	D	t	D/t	Crack	Dent	Notch
S5N1	168.25	8.33	20.20	44× 0.31 × 0.70	110× 80 × 10	44× 9.5 × 3.0
S5N2	168.80	7.60	22.21	44× 0.31 × 0.70	110× 80 × 10	44× 10 × 3.0

3.1. Comparison of simulation results

Both the structure failure mode and failure location have a good agreement with each other, as illustrated in Fig. 5. Due to the occurrence of combined damage, the failure of the pipe specimen initiates in the damaged region. The largest lateral displacement of the damaged pipe cross-section has not been compared due to a lack of test data.

The comparisons of the bending moment-curvature diagrams between tests and numerical results are shown in Fig. 6. The corresponding geometry and results of the specimens are listed in Tables 1 and 2, respectively. Both specimens (S5N1 and S5N2) have a combined dent and notch with 90º on the pipe compression side, as shown in Fig. 4. The occurrence of combined damage has induced a rapid failure of the specimens. Once the bending moment has reached the peak point, it decreases quickly with a further increase of curvature in almost a linear tendency until the termination of the test. The early scatter in the elastic domain of the curves indicates that there is a discrepancy of elastic modulus between the test and the simulation, where the default value for seamless steel is used as 2.06×10^5 MPa in this paper.

The comparison results in terms of critical bending moment (M_{cr}) and curvature (κ_{cr}) are listed in Table 2. It is observed that a good agreement in the critical bending moment has been reached, i.e., less than 2.2% discrepancy. Meanwhile, the results of critical curvature from the simulation have overestimated the deformation capacity of specimens. This is likely attributed to the factors of the material properties and the measurement method for curvature in the test.

4. Investigation of residual stress

Two types of residual stress exist in pipes, including the residual stress induced by manufacture workmanship and the residual stress induced by mechanical interference [15,16,21–24]. Due to the lack of test data for residual stress induced by mechanical interference, we only carry out simulations into the effect of residual stress on pipe residual ultimate strength with a specific stress distribution. An assumption of a linear distribution of the residual stress is used based on the survey from literature about residual stress tests [15,22–24]. Hence, the research in this section could be considered as an initial exploration for the impact induced residual stress.

4.1. Distribution of residual stress

As illustrated in Fig. 7, three different types of residual stress on pipes have been found. For the spiral-welded pipe developed by a cold bending manufacture process [15,16], it has a tensile residual stress on the inner surface and a compression stress on the outer surface in pipe hoop direction. Due to the occurrence of weld seams, the stress component in hoop direction has several turning points between compression and tension along the pipe thickness.

For seamless pipes produced by cold-drawing, residual stress presents a monotonical state with a much smaller value. As shown in Fig. 7(b) [24], the residual stress component in the hoop direction (equal to the Tangential direction in Fig. 7(b)) changes from compression on the inner surface to tension on the outer surface. The axial component changes from a strong compression on the inner surface to tension on the outer surface. The residual stress in the radial direction is small, varying from 0 on the inner surface to a slight compression on the outside of pipe. For seamless pipes produced by hot-rolling, the residual stress component in the hoop direction also presents a monotonical increase/decrease state, as shown in Fig. 7(c). In the test from Amirat et al. [23] on a typical API X60 seamless steel pipe, it is measured that there is a compression stress component in the hoop direction on the outside layer of seamless pipes, monotonical decrease until the largest tensile stress on the inside layer of pipes. The maximum residual stress is approximately 10% of the material yield stress. For the stress component in axial direction, it is generally assumed to be invariant and small due to its slight change based on test observation.

4.2. Effect of residual stress

Based on the survey of stress in pipes (hot-rolling) described in the previous section, the residual stress is assumed only in the pipe hoop direction with a peak value of $\pm$ $10\%\sigma_y$ on the surface of pipes in a linear distribution. Residual stress on the outer surface of

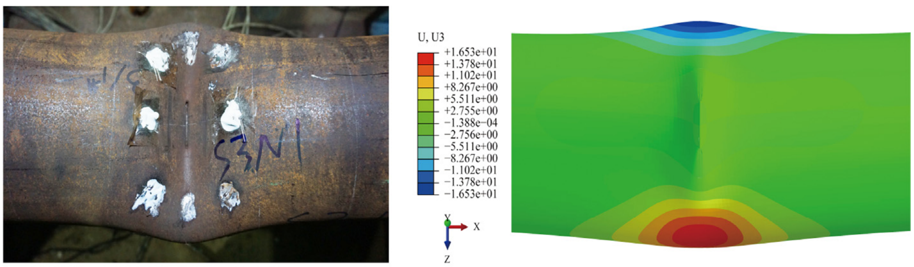

Failure mode in test   Failure mode in FEM

Fig. 5. Failure mode of specimen with combined damage.

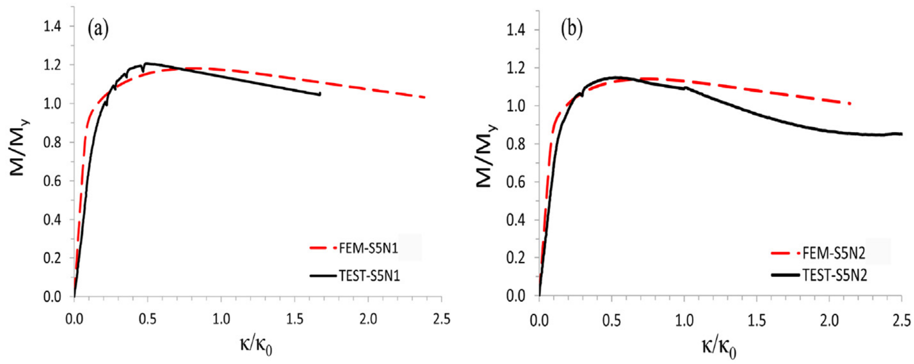

Fig. 6. Comparison between numerical and test results in terms of bending moment-curvature diagram: (a) specimen S5N1; (b) specimen S5N2.

Table 2
Comparison results of damaged specimens.

S.N.	M_{cr}(Test)	M_{cr}(FEA)	κ_{cr}(Test)	κ_{cr}(FEA)	error-M	error-κ
	(kNm)	(kNm)	(1/m)	(1/m)	(%)	(%)
S5N1	97.173	95.12	0.163	0.264	−2.11	61.96
S5N2	85.72	85.21	0.153	0.218	−0.59	42.48

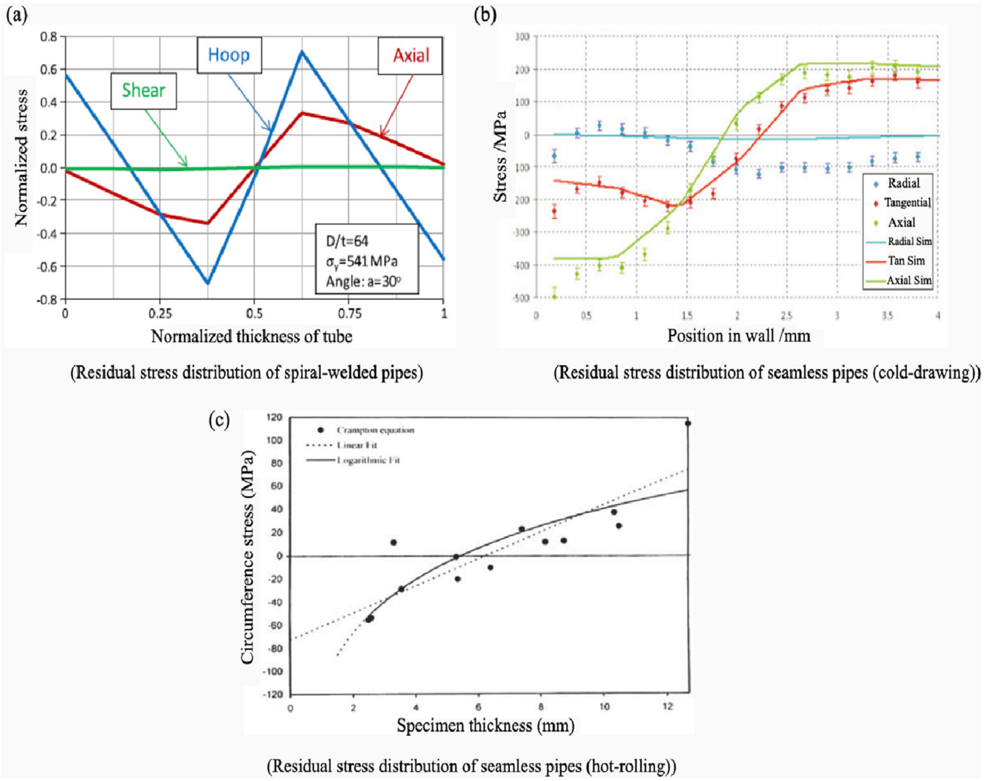

Fig. 7. Typical residul stress distribution of different types of intact pipes: (a) spiral-welde pipes (image from Ref. [16]); (b) seamless pipes by cold-drawing (image from Ref. [24]); (c) seamless pipes by hot-rolling (image from Ref. [23]).

pipes is in compression (− 34.5MPa), while the stress on pipe inner surface is in tension (34.5MPa). The type of structural damage on pipes is separated during simulations in order to have a comprehensive insight in the effect of residual stress.

Fig. 8 illustrates the normalized residual strength in terms of M_{cr}/M_y and κ_{cr}/κ_y with respect to different wrinkling imperfection (δ_0/t) for an intact pipe. The range of the initial imperfection amplitude is between 0 and $0.2t$. If the results between the pipes without

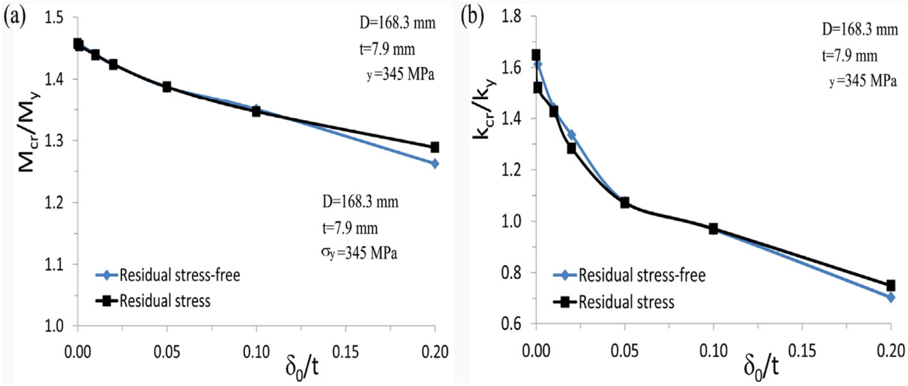

Fig. 8. Normalized residual strength (M_{cr}/M_y, κ_{cr}/κ_y) with respect to wrinkling imperfection (δ_0/t) for an intact pipe (Effect of residual stress).

residual stress and the pipes with residual stress are compared, then it is found that the residual stress only slightly affects the pipe strength. With the increase of imperfection, the residual stress presents a small retardation effect on the strength capacity.

When structural damage is preset on the pipe surface, different phenomena happen. Fig. 9 shows the effect on pipes with a dent. The dent depth varies between $0.2t$ and $2t$ with a fixed dent width (60 mm) and a dent length (100 mm) in the pipe hoop direction. The numerical results demonstrate a large increase of strength capacity accounting for residual stress when the dent depth is smaller than the pipe thickness t. With the further increase of the dent depth ($t < d_d \leq 2t$), such retardation effect is shielded due to the large damage effect. It is likely because of the fact that the occurrence of the compression residual stress on the pipe outer surface postpones its yielding, and then the loss of bending stiffness. When there is only a notch on pipes, it is found that the residual stress can seldom affect pipe strength, as illustrated in Fig. 10. No obvious differences have been observed based on the numerical results. The occurrence of a notch has completely shielded the effect of residual stress.

A positive effect on the pipe strength, from assumed residual stress, has been obtained accordingly, especially for intact pipes with a large initial imperfection (δ_0 no less than $0.2t$) and dented pipes with small dent depth ($d_d \leq t$). The effect of residual stress is shielded and becomes insignificant with the further increase of damage dimensions. Hence, it is reasonable not to account for the residual stress during the study of residual ultimate strength under this circumstance, which represents a more severe situation.

5. Simulation results of combined damage and proposed formulas

In this section, numerical simulations on damaged pipes are carried out based on the validated model, changing the geometrical size of each type of damage. The geometrical dimensions of used pipes for investigation are listed in Tables 3–7 with the same outer diameter of 168.80 mm. The same material properties from the material tensile test of the authors [1] are used, having a yield stress of 378 MPa, an ultimate tensile stress of 542 MPa and the maximum elongation of 24.6%. As discussed in Section 4, the residual stress has not been taken into account here, which represents a more severe situation.

In the following investigation, both the notch depth (d_m) and the dent depth (d_d) are normalized by the pipe thickness t. The simulation results in bending moment-curvature diagrams are normalized by M_y and κ_0, as described in Section 3. The results in terms of critical bending moment and critical curvature are normalized by their corresponding pipes without structural damage (M_i and κ_i). Therefore, reference values for G1 in simulation are 98.33 kNm and 0.567 $1/m$, while reference values for the other groups are 99.71 kNm and 0.579 $1/m$. The reference value for the test are 102.71 kNm and 0.401 $1/m$ based on the intact specimen S1N4 [1].

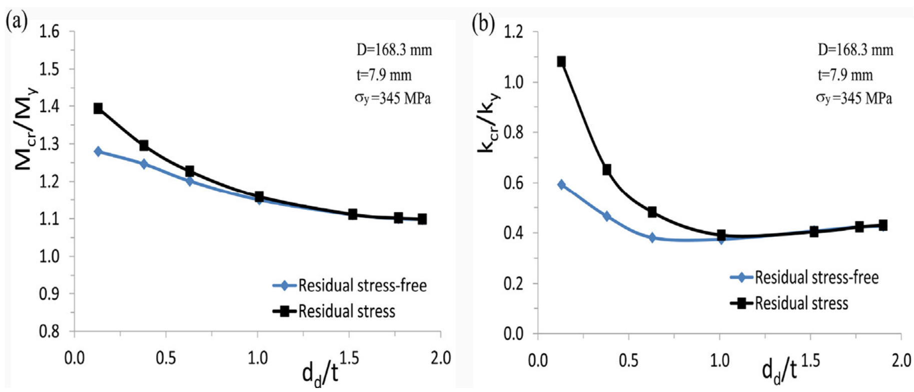

Fig. 9. Normalized residual strength (M_{cr}/M_y, κ_{cr}/κ_y) with respect to dent depth (d_d/t) for a dented pipe (Effect of residual stress).

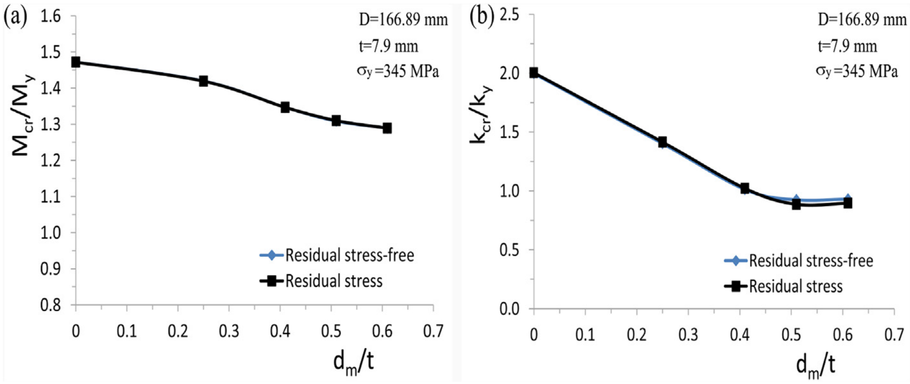

Fig. 10. Normalized residual strength (M_{cr}/M_y, κ_{cr}/κ_y) with respect to notch depth (d_m/t) for a pipe with notch (Effect of residual stress).

Table 3
Residual ultimate strength of pipes with varying of dent (G1, fixed notch).

Capacity	$t = 7.5$ mm											
	$l_m = 44$ mm, $w_m = 10$ mm, $d_m = 1.5$ mm											
	d_d/t											
G1	0.00	0.07	0.20	0.33	0.47	0.60	0.73	0.87	1.00	1.13	1.27	2.00
M_{cr}/M_i	0.980	0.955	0.916	0.886	0.862	0.844	0.830	0.820	0.811	0.804	0.798	0.778
κ_{cr}/κ_i	0.804	0.656	0.487	0.402	0.358	0.337	0.335	0.330	0.333	0.326	0.330	0.362

Table 4
Residual ultimate strength of pipes with varying of dent (G2, fixed notch).

Capacity	$t = 7.6$ mm											
	$l_m = 44$ mm, $w_m = 10$ mm, $d_m = 3.0$ mm											
	d_d/t											
G2	0.00	0.07	0.20	0.33	0.46	0.59	0.72	0.86	0.99	1.12	1.25	1.97
M_{cr}/M_i	0.918	0.902	0.875	0.854	0.838	0.826	0.816	0.808	0.802	0.796	0.792	0.776
κ_{cr}/κ_i	0.522	0.461	0.397	0.370	0.345	0.342	0.337	0.340	0.344	0.345	0.349	0.368

Table 5
Residual ultimate strength of pipes with varying of dent (G3, fixed notch).

Capacity	$t = 7.6$ mm											
	$l_m = 44$ mm, $w_m = 10$ mm, $d_m = 4.5$ mm											
	d_d/t											
G3	0.00	0.07	0.20	0.33	0.46	0.59	0.72	0.86	0.99	1.12	1.25	1.97
M_{cr}/M_i	0.878	0.868	0.850	0.836	0.825	0.815	0.807	0.801	0.796	0.792	0.788	0.773
κ_{cr}/κ_i	0.465	0.440	0.408	0.383	0.378	0.371	0.364	0.368	0.358	0.361	0.363	0.380

Two strategies are used for the following simulations. The first one is to change the dent depth (d_d) whilst a moderate metal loss in terms of a notch with a fixed dimension is preset, as shown in Fig. 11. As shown in Tables 3–5, the normalized dent depth (d_d/t) varies between 0 and 2.0 under three different types of specific notch ($d_m/t = 0.2$, $d_m/t = 0.4$ and $d_m/t = 0.59$). Hence, they are categorized as groups $G1$, $G2$ and $G3$. The second one is to change the notch depth (d_m) whilst a moderate dent with a fixed dimension is preset, as shown in Fig. 12. As shown in Tables 6 and 7, the normalized notch depth (d_m/t) varies between 0 and 0.62 under two different types of specific dent ($d_d/t = 1.32$ and $d_d/t = 0.66$). Hence, they are categorized as groups $G4$ and $G5$.

Table 6
Residual ultimate strength of pipes with varying of notch (G4, fixed dent).

Capacity	t = 7.6 mm											
	l_d = 120 mm, w_d = 60 mm, d_d = 10 mm											
	d_m/t											
G4	0.00	0.20	0.24	0.28	0.32	0.36	0.39	0.43	0.47	0.51	0.55	0.62
M_{cr}/M_i	0.790	0.784	0.782	0.780	0.779	0.777	0.776	0.775	0.774	0.773	0.772	0.771
κ_{cr}/κ_i	0.326	0.335	0.330	0.342	0.342	0.344	0.344	0.344	0.344	0.356	0.356	0.358

Table 7
Residual ultimate strength of pipes with varying of notch (G5, fixed dent).

Capacity	t = 7.6 mm							
	l_d = 120 mm, w_d = 60 mm, d_d = 5 mm							
	d_m/t							
G5	0.00	0.20	0.28	0.36	0.43	0.51	0.59	0.62
M_{cr}/M_i	0.845	0.830	0.821	0.814	0.807	0.803	0.800	0.800
κ_{cr}/κ_i	0.329	0.329	0.322	0.328	0.341	0.343	0.357	0.357

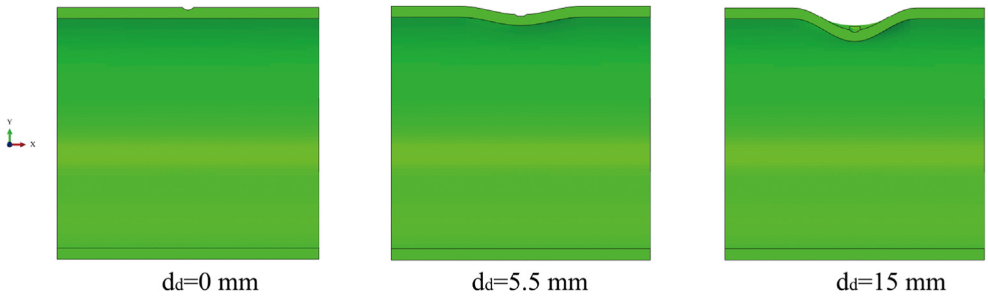

Fig. 11. Images of varied dent depth with a fixed notch in combined damage.

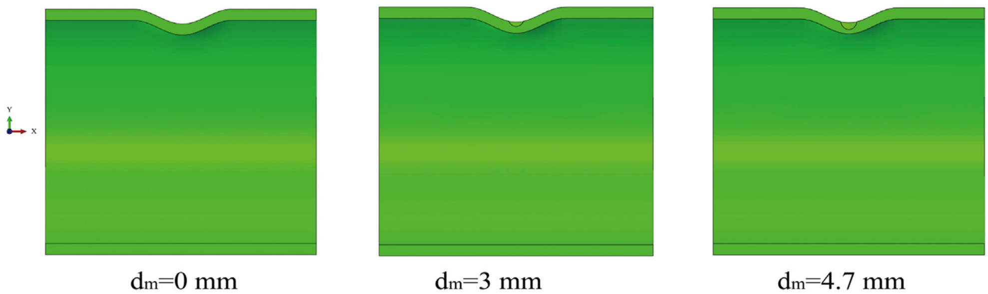

Fig. 12. Images of varied notch depth with a fixed dent in combined damage.

5.1. Effect of damage

Fig. 13 presents the normalized bending moment-curvature diagrams with the variation of dent depth in a combined damage. The "Intact-fixed-notch-G1" denotes the corresponding pipe case without any structural damage, while the "Dent-free" denotes the case with only notch damage. The following notations for notch are the same. A single notch significantly decreases the pipe strength capacity. It is observed that, under all the three types of notch, the occurrence of a dent further decreases the pipe strength largely. However, such further decrease is relative small with the increase of dent depth (d_d/t from 0.07 to 2.0).

Fig. 14 shows the normalized bending moment-curvature diagrams with the variation of the notch depth in a combined damage. Compared with the fixed notch cases in Fig. 13, an interesting phenomenon can be observed. Once a dent damage occurs on a pipe,

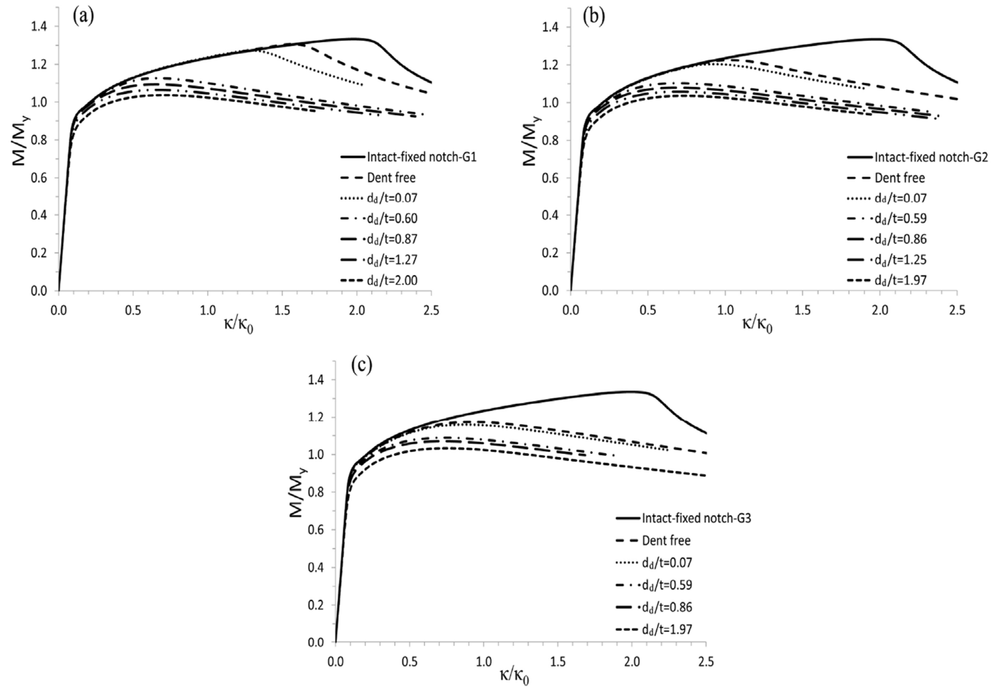

Fig. 13. Normalized bending moment-curvature diagrams with varying of dent depth in combined damage: (a) diagrams with fixed notch in G1 ($l_m = 44mm$, $w_m = 10mm$, $d_m = 1.5mm$); (b) diagrams with fixed notch in G2 ($l_m = 44mm$, $w_m = 10mm$, $d_m = 3.0mm$); (c) diagrams with fixed notch in G3 ($l_m = 44mm$, $w_m = 10mm$, $d_m = 4.5mm$).

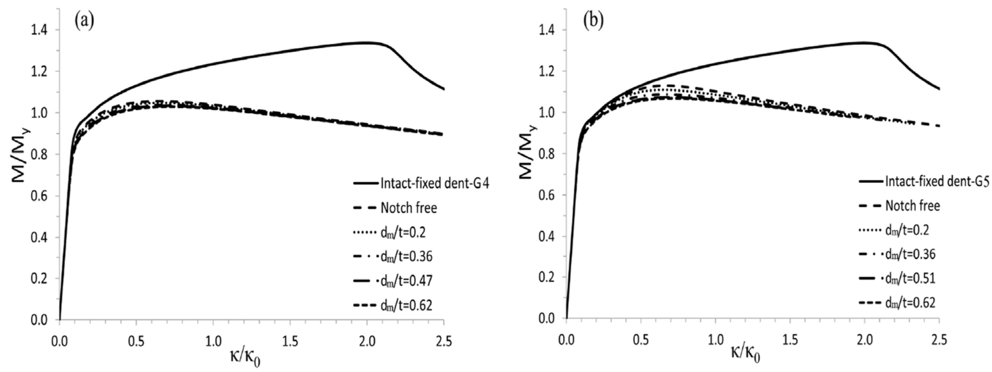

Fig. 14. Normalized bending moment-curvature diagrams with varying of notch depth in combined damage: (a) diagrams with fixed dent in G4 ($l_d = 120mm$, $w_d = 60mm$, $d_d = 10mm$); (b) diagrams with fixed dent in G5 ($l_d = 120mm$, $w_d = 60mm$, $d_d = 5mm$).

further increase of the severity of notch in terms of the notch depth (d_m/t from 0.2 to 0.62) only has slight effect on the residual strength. Therefore, we can come to the conclusions that the type of combined damage has a more severe effect on the pipe residual strength compared to a single type of damage, and the dent damage plays a more dominant role on pipe residual strength in the combined dent and notch damage.

5.2. Proposed formulas

In the former research of the authors, empirical formulas are proposed for each type of structural damage, taking into account their relevant critical damage parameters. For a pipe with a single plain dent in its central cross-section under a bending moment, the empirical formulas have been proposed and can be written as [4]:

$$\left(\frac{M_{cr}}{M_i}\right)_d = 1 - a_1\left(\frac{d_d}{t}\right)^{b_1}(\lambda_l)^{c_1} \tag{1}$$

$$\left(\frac{\kappa_{cr}}{\kappa_i}\right)_d = 1 - \left(a_2 + b_2\frac{t}{d_d}\right)(\lambda_l)^{c_2} \tag{2}$$

Where a_1, b_1 and c_1 are 0.017, 0.696 and 1.48, respectively; a_2, b_2 and c_2 are 0.192, -0.026 and 0.955, respectively. Parameter λ_l here is the normalized dent length in the pipe hoop direction ($\lambda_l = l_d/\sqrt{Rt}$, $\lambda_l \in [0.8, 5.2]$), while d_d/t is the normalized dent depth which is between 0.1 and 2.2. The normalized dent width λ_w should be in the range between 1.0 and 3.17 due to the former research from the authors [4].

Meanwhile, for a pipe with a single notch in its central cross-section under bending moment, the empirical formulas can be written as [5]:

$$\left(\frac{M_{cr}}{M_i}\right)_m = 1 - a_3\left(\lambda_l\frac{d_m}{t}\right)^{b_3}(\lambda_w)^{c_3} \tag{3}$$

$$\left(\frac{\kappa_{cr}}{\kappa_i}\right)_m = 1 - a_4\left(\lambda_l\frac{d_m}{t}\right)^{b_4}(\lambda_w)^{c_4} \tag{4}$$

Where a_3, b_3 and c_3 are 0.139, 0.91 and 0.253, respectively; a_4, b_4 and c_4 are 0.652, 0.557 and 0.205, respectively. Parameter λ_l is the normalized notch length in pipe hoop direction ($\lambda_l = l_m/\sqrt{Rt}$, $\lambda_l \in [0.2, 4.8]$), while λ_w is the normalized notch width in pipe longitudinal direction ($\lambda_w = w_m/\sqrt{Rt}$, $\lambda_l \in [0.3, 1.4]$). d_m/t is the normalized notch depth which is between 0.2 and 0.65 based on the former research [5].

For the combined dent and notch damage, there may be a coupling effect between each damage, which is difficult to obtain directly. Therefore, in this paper, we first construct the form of prediction formulas in the functions of individual damage effect, as seen in Eqs. (5) and (6). Where $(M_{cr}/M_i)_m$ and $(\kappa_{cr}/\kappa_i)_m$ are the reduction ratios due to a single notch, which can be calculated by Eqs. (3) and (4) respectively; $(M_{cr}/M_i)_d$ and $(\kappa_{cr}/\kappa_i)_d$ are the reduction ratios due to a single dent, which can be calculated by Eqs. (1) and (2) respectively. Through the corresponding numerical simulation results on pipes with combined damage (Tables 3–7), a regression analysis on the constructed formulas (Eqs. (5) and (6)) is carried out.

$$\left(\frac{M_{cr}}{M_i}\right)_{com} = a_5\left(\frac{M_{cr}}{M_i}\right)_m + b_5\left(\frac{M_{cr}}{M_i}\right)_d + c_5 \tag{5}$$

$$\left(\frac{\kappa_{cr}}{\kappa_i}\right)_{com} = a_6\left(\frac{\kappa_{cr}}{\kappa_i}\right)_m^2 + b_6\left(\frac{\kappa_{cr}}{\kappa_i}\right)_d^2 + c_6\left(\frac{\kappa_{cr}}{\kappa_i}\right)_m + d_6\left(\frac{\kappa_{cr}}{\kappa_i}\right)_d + e_6\left(\frac{\kappa_{cr}}{\kappa_i}\right)_m\left(\frac{\kappa_{cr}}{\kappa_i}\right)_d + f_6 \tag{6}$$

Where the corresponding coefficients a_5, b_5 and c_5 are 0.338, 0.566 and 0.016 respectively, and a_6, b_6, c_6, d_6, e_6 and f_6 are 0.251, 0.299, -0.653, -0.605, 0.828 and 0.647 respectively for the quadratic polynomial Eq. (6).

In order to determine the model uncertainty, we use the same method as the one in the former research [5,25]. The definition of X can be written as $X = X_{true}/X_{predict}$, where X_{true} is the data from either experimental test or numerical simulation, $X_{predict}$ is the prediction values due to proposed equations. Both X_{true} and $X_{predict}$ are assumed from the same cases with the same material properties and geometry. Table 8 shows the statistical results of X in terms of the mean value (bias) and coefficient of variation (COV, defined as the ratio of the standard deviation to the mean value of data). Due to the limited number of tests, comparison with test results has not been statistically carried out here. Results show that the extent of variability for the prediction of M_{cr} is within 1.28%, while the extent of variability for the prediction of κ_{cr} is within 3.33%. Furthermore, Fig. 15 shows the results of the comparison between predictions, test and numerical simulations. An underestimation from the formulas has been obtained compared with the test results.

Fig. 16 presents the prediction results of metallic pipes with combined damage with respect to the varying of different damage (d_d/t for dent, d_m/t for notch). Analysis of variance (ANOVA) shows that R square of the fitted formulas are 0.917 and 0.902 respectively, which demonstrated a high accuracy of the prediction from the proposed formulas.

5.3. Expansion of the application domain of formulas

In practice, when mechanical interference happens, the proposed formulas in Section 5.2 can be used to predict the residual ultimate strength of metallic pipes with combined damage under dominant bending. An on-site geometrical measurement should be first carried out for individual damage (a dent and/or a notch). By using the prediction formulas based on the former research of the authors [4,5], the specific effect of single type of damage can be first calculated. Substituting all these data into Eqs. (5) and (6), we can then find a final estimation of the effect of the combined damage.

Table 8
Model uncertainties of the proposed formulas.

X	Moment, Eq. (5)		Curvature, Eq. (6)	
	Mean (Bias)	COV	Mean (Bias)	COV
FEM	1.0000	0.0128	1.0001	0.0333

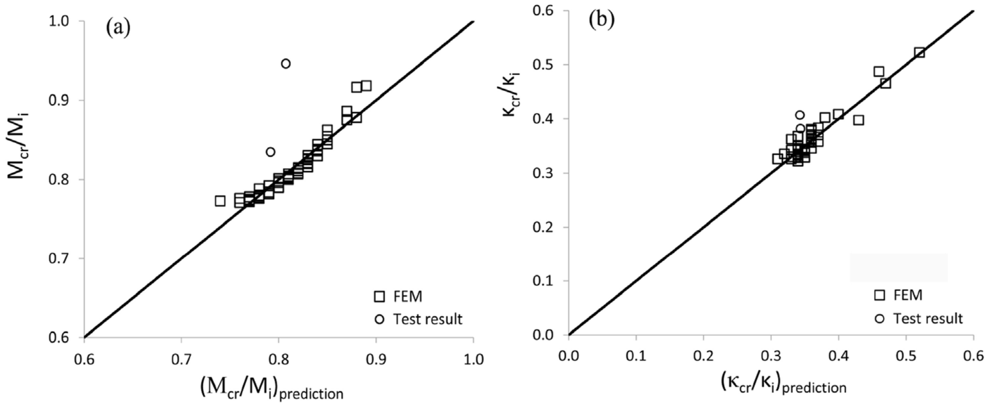

Fig. 15. Comparison between prediction of proposed equations and experimental, numerical results and analytical results: (a) Normalized residual ultimate moment (M_{cr}/M_i); (b) Normalized critical curvature (κ_{cr}/κ_i).

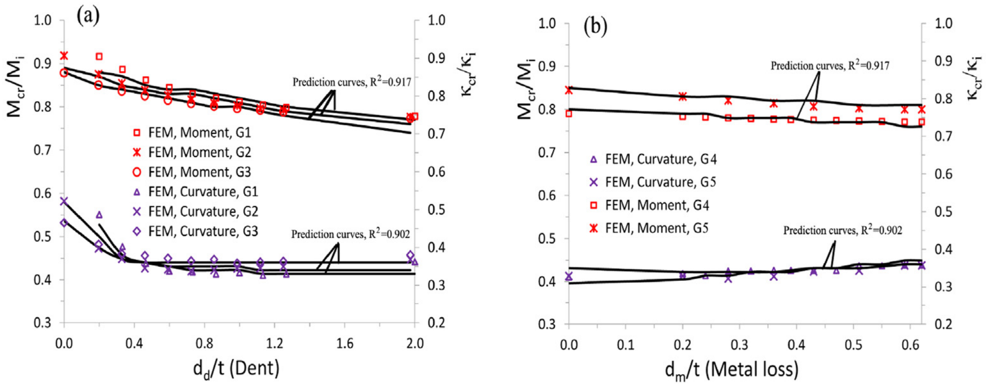

Fig. 16. Prediction of damaged metallic pipes with respet to the varying of damage: (a) fixed notch with varying of dent; (b) fixed dent with varying of notch.

As discussed above, the prediction formulas are proposed based on a specific type of pipe with D/t around 21. In order to expand the application domain of the formulas, extra numerical simulations with varying of D/t (from 15 to 50) are carried out. A fixed pipe diameter of 168.8 mm is used with a change of pipe thickness to obtain different D/t. A combined damage with fixed dimension is introduced on the pipe surface, including the dent size of $l_d \times w_d \times d_d = 120 \times 60 \times t\ \ mm$ and the notch size of $l_m \times w_m \times d_m = 44 \times 10 \times 0.4t\ mm$. Therefore, the simulation results from both the intact pipes and the damaged pipes with different D/t are listed in Tables 9 and 10. As demonstrated from the bending moment-curvature diagrams in three types of pipes in Fig. 17, the failure modes begin to present differences in case with $D/t = 29$. In the case with $D/t = 50$, rapid failure of structures occurs with an abrupt degradation. Hence, the change of failure modes could affect the reduction ratio of strength on damaged pipes with different D/t.

A further comparison of the predictions and the numerical results in different D/t ratios is shown in Fig. 18. As can be seen in Fig. 18(a), the proposed formula can also provide a good prediction on critical moment for pipes with D/t from 15 to 50. A little bit underestimation of the strength is introduced in pipes with $D/t = 50$, with the maximum discrepancy of 5.7%. For the prediction of critical curvature, an underestimation is introduced for cases with D/t less than 25, which is on a safety zone. However, with the

Table 9
Residual ultimate strength of intact pipes with varying of diameter-to-thickness ratios.

Capacity	$D = 168.8\ mm$, No imperfection, $\sigma_y = 378MPa$						
D/t	15	17	19	23	25	27	29	32
$M_i(MPa)$	149.73	131.78	117.38	96.11	87.94	80.99	70.09	67.6
$\kappa_i(1/m)$	1.048	0.866	0.733	0.529	0.484	0.435	0.306	0.331
D/t	35	38	41	44	47	50		
$M_i(MPa)$	61.25	56.03	51.66	47.85	44.46	41.62		
$\kappa_i(1/m)$	0.287	0.251	0.225	0.204	0.184	0.166		

Table 10
Residual ultimate strength of damaged pipes with varying of diameter-to-thickness ratios.

Capacity	$D = 168.8$ mm, $l_d = 120$ mm, $w_d = 60$ mm, $d_d = t$ mm						
	$l_m = 44$ mm, $w_m = 10$ mm, $d_m = 0.4 \times t$ mm						
D/t	15	17	19	23	25	27	29	32
M_{cr}/M_i	0.826	0.821	0.800	0.785	0.777	0.764	0.818	0.765
κ_{cr}/κ_i	0.443	0.420	0.514	0.344	0.320	0.294	0.369	0.281
D/t	35	38	41	44	47	50		
M_{cr}/M_i	0.750	0.744	0.739	0.735	0.733	0.732		
κ_{cr}/κ_i	0.275	0.271	0.271	0.216	0.201	0.217		

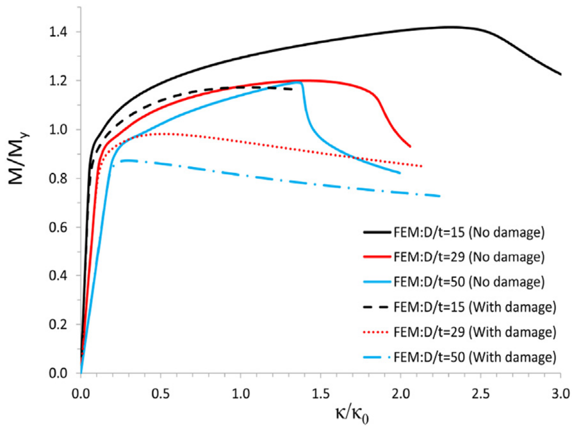

Fig. 17. Normalized bending moment-curvature diagrams with varying of pipe diameter-to-thickness ratios (D/t is 15,29 and 50 respectively).

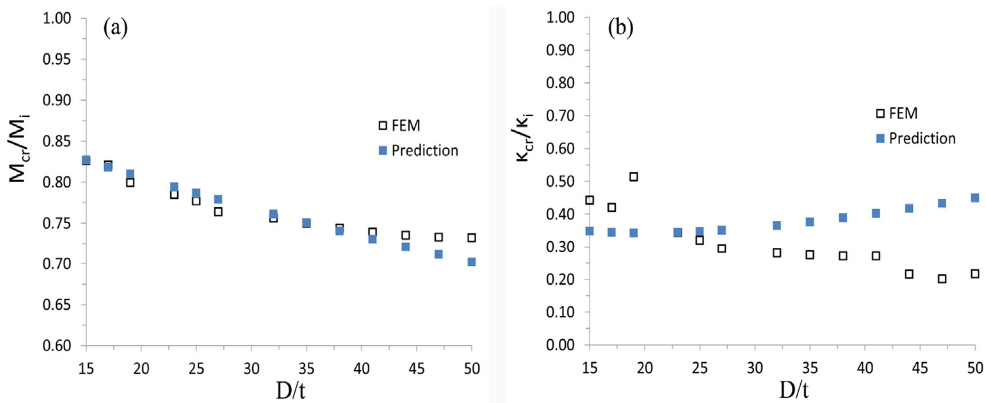

Fig. 18. Comparison results between prediction and numerical results on pipes with varying of D/t: (a) normalized critical moment; (b) normalized critical curvature.

increase of D/t, an overestimation of the critical curvature is introduced, as can be seen in Fig. 18(b). The larger the D/t is, the larger the discrepancy from the prediction will be. In sum, accounting for the valid application domain of each damage parameter for pipes with the single type of damage, we consider that the proposed formulas in this paper can be also used for damaged pipes with D/t up to 30. In spite of such reasonable expansion, further tests are needed to confirm the validity of the formulas.

6. Conclusions

As a consecutive study, this paper has provided an extensive numerical investigation in the residual ultimate strength of damaged seamless pipes that suffered from combined dent and metal loss. A simplified numerical model accounting for combined structural damage has been developed and validated. The effect of residual stress has been initially explored to consider the impact effect. The conclusions of this paper are drawn as follows:

1. The developed numerical model accounting for combined dent and notch damage is capable of providing an accurate prediction of the bending behavior in terms of critical bending moment and failure mode. The prediction of critical curvature overestimates the deformation capacity of the test specimens.
2. The residual stress in the assumed distribution in this paper provides a positive effect on the pipe strength, especially for intact pipes with large initial imperfection (δ_0 no less than $0.2t$) and dented pipes with small dent depth ($d_d \leq t$). Due to the occurrence of large structural damage, the effect of residual stress is shielded and becomes insignificant. Further studies on residual stress are needed based on the real distribution from impact tests.
3. The combined dent and notch damage has a more severe effect on the pipe residual strength compared with other types of damage (excluding the possible fracture failure). The dent damage plays a more dominant role on the pipe residual strength compared with the notch in the combined damage.
4. Empirical formulas are proposed to predict the residual ultimate strength of metallic pipes with combined damage under a bending moment. These formulas could be utilized for practice purposes through a simple on-site measurement, which will facilitate the decision-making of pipe maintenance after mechanical interference. The proposed formulas in this paper are only based on a certain type of metallic pipes with D/t around 21. However, the application domain has been extended to damaged pipes with D/t up to 30 through further simulation. Further tests are still required in order to confirm the validity of such an expansion of the application domain.

Acknowledgments

Thanks to the financial support of China Scholarship Council (CSC) [grant number 2014062 30001]. The funding for the tests that was provided by the Section of Transport Engineering and Logistics, Department of Maritime and Transport Technology, Delft University of Technology, the Netherlands, and the School of Transportation of Wuhan University of Technology, PR China, is also appreciated.

References

[1] Cai J, Jiang XL, Lodewijks G, Pei ZY, Zhu L. Experimental investigation of residual ultimate strength of damaged metallic pipelines. ASME 2017 36th international conference on offshore mechanics and arctic engineering. American Society of Mechanical Engineers; 2017.
[2] Cai J, Jiang XL, Lodewijks G. Residual ultimate strength of offshore metallic pipelines with structural damage–a literature review. Ships Offshore Struct 2017:1–19.
[3] Cai J, Jiang XL, Lodewijks G. Numerical investigation of residual ultimate of dented metallic pipes subjected to pure bending. Ships Offshore Struct 2018;13(5):519–31.
[4] Cai J, Jiang XL, Lodewijks G, Pei ZY, Wu WG. Residual ultimate strength of seamless metallic pipelines – a numerical investigation (accepted with revision). Ocean Eng 2018.
[5] Cai J, Jiang XL, Lodewijks G, Pei ZY, Wu WG. Residual ultimate strength of damaged seamless metallic pipelines with metal loss. Mar Struct 2018;58:242–53.
[6] Manes A, Porcaro R, Ilstad H, Levold E, Langseth M, Børvik T. The behaviour of an offshore steel pipeline material subjected to bending and stretching. Ships Offshore Struct 2012;7(4):371–87.
[7] Ghaednia H, Das S, Wang R, Kania R. Safe burst strength of a pipeline with dent–crack defect: effect of crack depth and operating pressure. Eng Fail Anal 2015;55:288–99.
[8] Zhang S, Pedersen PT, Ocakli H. Collisions damage assessment of ships and jack-up rigs. Ships Offshore Struct 2015;10(5):470–8.
[9] PHMSA. Pipeline incident 20 year trend Tech. rep. U.S.Department of Transportation; 2017.
[10] Bjørnøy O, Rengård O, Fredheim S, Bruce P. Residual strength of dented pipelines, DNV test results. The tenth international offshore and polar engineering conference. International Society of Offshore and Polar Engineers; 2000.
[11] DNV. DNV-RP-F111:Interference between trawl gear and pipelines. latest ed. Det Norske Veritas; 2010.
[12] Park T, Kyriakides S. On the collapse of dented cylinders under external pressure. Int J Mech Sci 1996;38(5):557–78.
[13] Levold E, Marchionni L, Vitali L, Molinari C, Restelli A, Ozkan IF. Strength and deformation capacity of corroded pipe-laboratory tests and FEM analyses. The twenty-third international offshore and polar engineering conference. International Society of Offshore and Polar Engineers; 2013.
[14] Bai Y, Bai Q. Subsea pipeline integrity and risk management. Gulf Professional Publishing; 2014.
[15] Es S, Gresnigt AM, Vasilikis D, Karamanos SA. Ultimate bending capacity of spiral–welded steel tubes–part i: Experiments. Thin-Walled Struct 2016;102:286–304.
[16] Vasilikis D, Karamanos SA, Es S, Gresnigt AM. Ultimate bending capacity of spiral-welded steel tubes–part ii: Predictions. Thin-Walled Struct 2016;102:305–19.
[17] Abaqus6.13. Abaqus: user's manual 6.13. 2013.
[18] Cai J, Jiang XL, Lodewijks G. Residual strength of metallic pipelines subject to combined loads accounting for impact induced damage. The 26th international ocean and polar engineering conference. International Society of Offshore and Polar Engineers; 2016.
[19] Prabu B, Raviprakash A, Venkatraman A. Parametric study on buckling behaviour of dented short carbon steel cylindrical shell subjected to uniform axial compression. Thin-Walled Struct 2010;48(8):639–49.
[20] GB/T 1591. High strength low alloy structural steels (in Chinese). latest ed. The Chinese National Standard; 2008.
[21] Lynch J. The measurement of residual stresses. Cleveland, OH: American Society for Metals, Residual Stress Measurements; 1952. p. 42–96.
[22] Sorem Jr. J, Shadley J, Rybicki E. Experimental method for determining through thickness residual hoop stresses in thin walled pipes and tubes without inside access. Strain 1990;26(1):7–14.
[23] Amirat A, Chaoui K, Azari Z, Pluvinage G. Residual stress analysis in seamless api x60 steel gas pipelines. Sci Technol B 2004:7–10.
[24] Pirling T, Carradò A, Palkowski H. Residual stress distribution in seamless tubes determined experimentally and by fem. Procedia Eng 2011;10:3080–5.
[25] Bai Y, Igland RT, Moan T. Ultimate limit states of pipes under tension and bending. Int J Offshore Polar Eng 1994;4(04).